



# OPEN Assessment of pit viper associated subclinical myocardial injury by speckle tracking imaging

Jing Chen<sup>1,2,6</sup>, Yang Feng<sup>1,6</sup>, Jiaqi Chen<sup>1</sup>, Chunmei Yin<sup>1</sup>, Jiaming Xia<sup>1</sup>, Li Fan<sup>1</sup>, Liqun Sun<sup>3,4</sup> & Chunjiang Yang<sup>1,5</sup>✉

In post-snakebite patient care, cardiac function is chiefly monitored through Left Ventricular Ejection Fraction (LVEF) via traditional echocardiography. This approach fails to detect early systolic dysfunction sensitively, which is key for managing envenomation-induced myocardial damage and impacts treatment and prognosis. In a study of 37 snakebite patients, individuals were grouped by severity using the Snakebite Severity Scale (SSS). Correlations between serological markers and two-dimensional speckle tracking echocardiography (2D-STE) strain parameters were analyzed, with ROC curves assessing the diagnostic effectiveness for myocardial injury. After a venomous snakebite, the study found a significant decrease in the left ventricular endocardial global longitudinal strain (GLSendo) compared to the middle and epicardium layer ( $p < 0.01$ ). The circumferential strain of the apical segment (ACS) was also lower in the affected group than in the control group ( $p < 0.05$ ), with more severe envenomation associated with a great reduction in both GLSendo and the ACS ( $p < 0.01$ ). The sensitivity of GLSendo for diagnosing myocardial injury due to venomous snakebite was 0.935, with the cut-off was 18.7%. The finding underscores the importance of using GLSendo as part of the standard echocardiographic assessment in patient. By providing early insight into the extent of myocardial injury and informed decisions regarding treatment and patient management.

**Keywords** Snake venom, Cardiotoxicity, Speckle tracking echocardiography, Myocardial injury, Left ventricular function

## Abbreviations

aCMQ Automated cardiac motion quantification  
RRSR Relative regional strain ratio

Snakebite envenomation, a significant global health concern with an estimated 5 million cases annually, results in substantial morbidity and mortality<sup>1</sup>. Venom-induced cardiotoxicity is a critical complication contributing to fatalities. Snake venom contains a complex mixture of biologically active molecules that primarily affect the nervous and cardiovascular system, with the incidence of cardiac involvement being about 0.2–3.8%<sup>2</sup>. A latent period between envenomation and cardiac symptoms underscores the need for early detection of cardiac involvement. While crucial, clinical assessments, including electrocardiograms (ECG) and myocardial markers<sup>3</sup>, may lack sensitivity and specificity. Advanced cardiac imaging modalities, such as Nuclear Imaging, and Cardiac Magnetic Resonance, offer more detailed evaluations but are limited by cost and accessibility. The employment of two-dimensional speckle tracking echocardiography (2D-STE) in this study for evaluating myocardial strain provides a sensitive, non-invasive tool for detecting early myocardial dysfunction post-snakebite, potentially guiding timely interventions and improving patient outcomes<sup>4</sup>.

<sup>1</sup>Department of Ultrasound, National Clinical Research Center for Child Health and Disorders, Ministry of Education Key Laboratory of Child Development and Disorders, China International Science and Technology Cooperation Base of Child Development and Critical Disorders, Chongqing Key Laboratory of Pediatric Metabolism and Inflammatory Diseases, Children's Hospital of Chongqing Medical University, Chongqing, China. <sup>2</sup>Ultrasonography Department, Chongqing Emergency Medical Center, Chongqing, China. <sup>3</sup>Department of Pediatrics, Division of Cardiology, The Hospital for Sick Children, University of Toronto, Toronto, Canada. <sup>4</sup>Translational Medicine Program, Research Institute, The Hospital for Sick Children, University of Toronto, Toronto, Canada. <sup>5</sup>Children's Hospital of Chongqing Medical University, Yuzhong District, Lianglukou Street, Chongqing, China. <sup>6</sup>Jing Chen and Yang Feng have contributed to the work equally and should be regarded as co-first authors. ✉email: cjyang@hospital.cqmu.edu.cn

LVEF is a well-recognized prognostic indicator in the general population<sup>5</sup>. However, its accuracy for early detection of cardiotoxicity is subject to debate<sup>6</sup>. 2D-STE offers a quantitative assessment of myocardial mechanical function through myocardial strain analysis, less influenced by loading conditions than conventional left ventricular systolic function like LVEF and fractional shortening (FS). Strain parameters can identify myocardial ischemia and infarction more sensitively and accurately, objectively reflecting overall and local functional changes<sup>7</sup>. The American Society of Echocardiography and the European Association of Cardiovascular Imaging have recognized global longitudinal strain (GLS) as the preferred deformation technique for early detection of subclinical left ventricular dysfunction<sup>8</sup>. Imaging methods for assessing cardiac function after venomous snake bite are underutilized. Circulatory failure frequently results from haematotoxic and mixed venom snake bites, predominantly inflicted by snakes belonging to the Viperidae family, which has a global distribution. Pit vipers, as part of the Viperidae family, are particularly noted for causing this condition. The primary cause is the potent histolytic, haemolytic, anticoagulant, and cardiotoxic effects of haematotoxins, which encompass cardiotoxins, cytotoxins, and haemorrhagic toxins. Notably, cardiotoxins constitute a significant portion, ranging between 20 and 40%, of the natural venom found in these snakes<sup>9</sup>. The study included the wild common viper “*Protobothrops mucrosquamatus*”, a species of *Agkistrodon halys*<sup>10</sup>, to analyze myocardial markers, ECG, conventional ultrasound parameters, and 2D-STE parameters in patients bitten by this pit viper. The initial investigation aimed to explore myocardial toxicity in snakebite patients using STE, and to evaluate its diagnostic value in assessing myocardial injury caused by snake venom.

## Methods

### Patient group

In this prospective investigation, executed from June 2022 through June 2023, a cohort of 50 patients, subsequent to pit viper envenomation, was admitted to our institution. The study was meticulously designed to evaluate the potential of STE in forecasting myocardial damage resultant from snake venom. Inclusion criteria mandated: 1) an unequivocal diagnosis of venomous snake bite, substantiated by cross-verification with a reptilian cadaver or representative imagery; 2) admission and initial consultation at our hospital within a 24-h window post-envenomation; 3) superior two-dimensional STE image resolution, characterized by a discernible left intraventricular membrane demarcation. Criteria for exclusion encompassed: 1) absence of envenoming, colloquially referred to as “dry bite”; 2) preceding pharmacological interventions, including antivenom administration or medications with cardiotoxic or cardioprotective properties; 3) pre-existing conditions conducive to cardiac compromise, such as systemic autoimmune disorders, diabetes mellitus, uremia, hyperthyroidism, and coronary arterial disease; 4) variables such as corpulence and emphysematous conditions that impair imaging fidelity. Subsequent to screening, five individuals were disqualified due to an inability to verify venomous snake bites, one patient had coronary artery disease, three patients exhibited no signs of poisoning, one patient’s admission transpired three days post-bite, contingent upon exacerbated clinical presentation, and three patients were disqualified owing to suboptimal echocardiographic image quality (Fig. 1). Consequently, the final cohort comprised 37 patients. Concurrently, to serve as a control assembly, 34 healthy adults were convened from our medical examination center, with gender and age judiciously matched to the experimental cohort. Institutional Review Board approval was obtained (Lot No. 2022-72). All experiments were performed in accordance with relevant named guidelines and regulations and all participants furnished written informed consent.

### Clinical characters and serologic markers

For each participant, demographic data including age, stature, mass, arterial pressure, pulse rate, and bite location were documented, and the body surface area was computed. ECG recordings were procured, and within a 24-h window post-admission, venous blood specimens were harvested from each patient. Hematologic analyses included the enumeration of white blood cells (WBC) and the quantification of C-reactive protein (CRP), cardiac troponin I (cTnI), and the comprehensive myocardial enzyme profile. The latter encompassed lactate dehydrogenase (LDH), creatine kinase (CK), the MB fraction of creatine kinase (CK-MB), and alpha-hydroxybutyrate dehydrogenase ( $\alpha$ -HBD). Concurrently, the clinical presentations pertinent to the respiratory and cardiovascular systems, localized trauma, gastrointestinal tract, hematopoietic system, and central nervous system were meticulously documented. Utilizing the SSS scale<sup>11</sup>, subjects were subsequently scored and categorized, with scores ranging from 0 to 3 indicative of mild manifestations, 4–7 signifying moderate severity, and 8–20 denoting severe involvement.

### Image acquisition

Echocardiographic assessments were consistently administered by the same physician employing an ultrasonographic device (Philips EPIQ5) equipped with a cardiac probe (S5-1), in strict adherence to prevailing guidelines<sup>12,13</sup>. Subsequent to ensuring the subjects’ repose in the left lateral decubitus position and facilitating calm respiration, ECG leads were attached, and arterial pressure was concurrently gauged. The primary sonographic acquisitions encompassed an M-mode echocardiogram via the parasternal long-axis visualization of the left ventricle, alongside the mitral annular motion spectra, ascertained through Tissue Doppler Imaging (TDI). A comprehensive interrogation of the left ventricular two-, three-, and four-chamber perspectives, in conjunction with the short-axis views at the mitral valve, papillary muscle, and apical tiers, were sequentially attained from the left ventricular apical long-axis vantage, ensuring representation across more than three cardiac cycles.

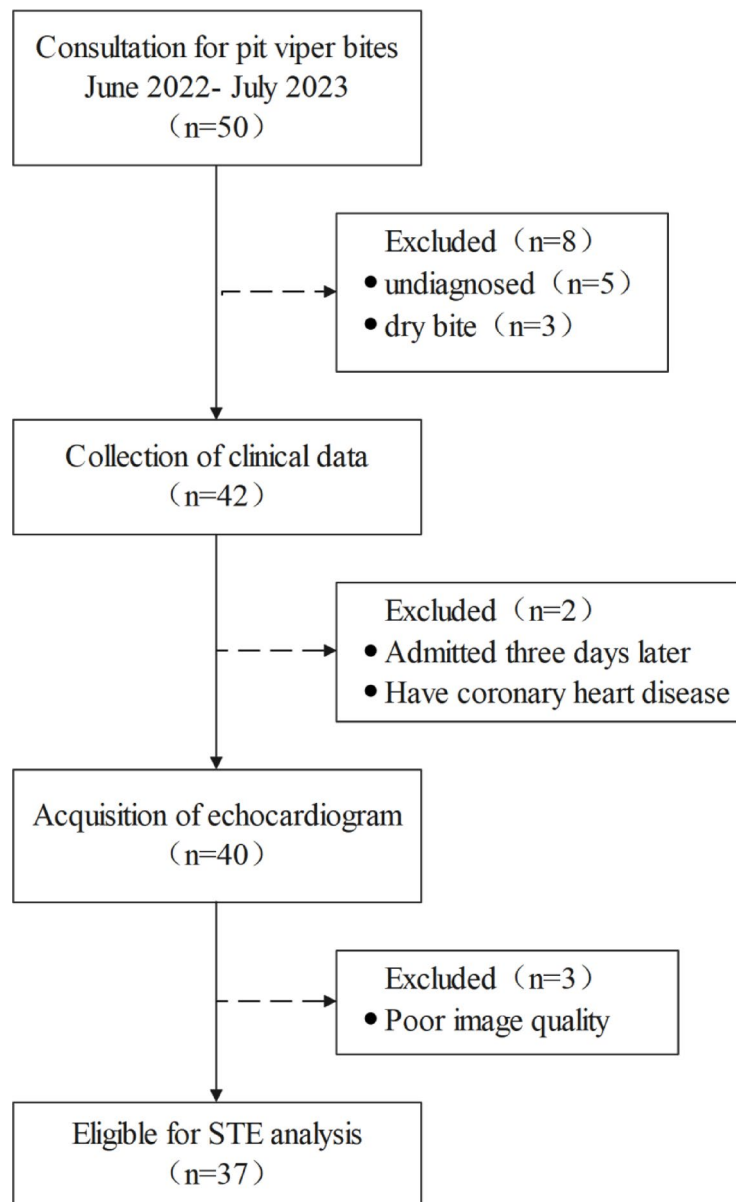


**Fig. 1.** Study flow chart. Abbreviations: STE, speckle tracking echocardiography.

### Quantitative echocardiographic analysis

Conventional echocardiographic parameters were meticulously recorded. The sonographic imagery was exported in DICOM format and subjected to analysis utilizing Philips offline software QLAB 13.0. The dynamic representation of left ventricular myocardial motion was manifested in both apical four-chamber and apical two-chamber perspectives. Via the biplane Simpson method, the left ventricular end-diastolic volume (LVEDV), left ventricular end-systolic volume (LVESV), and LVEF were ascertained. Peak mitral orifice flow velocities, delineated as peaks E and A, were gauged through spectral Doppler within the apical 4-chamber visualization, facilitating the derivation of the E/A ratio. Concurrently, peak anterior mitral annular motion velocities, demarcated as peaks e and a, were evaluated using tissue Doppler, thereby enabling the calculation of the E/e' and e'/a' ratios. Furthermore, the Tei index, which expresses the ratio of the amalgamated isovolumetric relaxation time and isovolumetric contraction time to the ejection time, was determined.

Left ventricular strain parameters were assessed using AutoStrain left ventricular mode, which automatically calculates the average of global longitudinal strain in the left ventricle (LVGLS) by tracing and tracking the ventricular membrane surface in view of three-chambered, four-chambered, and two-chambered (GLPS-A4C, GLPS-A3C, GLPS-A2C). In automated cardiac motion quantification (aCMQ) mode, manual delineation of each layer's endocardium was performed to measure endocardial global longitudinal strain (GLSendo), mid-layer myocardial global longitudinal strain (GLSmid), and epicardial myocardial global longitudinal strain (GLSepi). The mean longitudinal strain in the basal segment (BLS), middle segment (MLS), and apical segment (ALS) were recorded from bovine ophthalmogram derived from GLSendo. The relative regional strain ratio

(RRSR) was calculated using the formula:  $RRSR = ALS / (BLS + MLS)^{14}$ . Short-axis views at the mitral valve level, papillary muscle level, and apical segment level were traced to obtain the basal circumferential strain (BCS), middle circumferential strain (MCS), apical circumferential strain (ACS), and global circumferential strain (GCS).

Reproducibility analysis was conducted by assessing images of 5 randomly selected subjects from each of the 2 groups for interobserver major strain parameters (including GLPS-A4C, GLPS-A3C, GLPS-A2C, GLS, GLSendo, GLSmid, GLSepi, BCS, MCS, ACS, and GCS) consistency. Images from the same enrollee were measured again by the same sonographer after a 1-month interval to assess intra-observer consistency. The results were expressed as the intraclass correlation coefficient (ICC).

### Statistical analysis

Statistical analyses were conducted using SPSS 27.0 software, with all strain results being negative and presented in absolute values. Continuous variables were expressed as mean  $\pm$  standard deviation ( $\bar{x} \pm s$ ) or median (interquartile range). The normality of all data was assessed using the Shapiro–Wilk test. Variance analysis between the two groups was performed using the t-test for normally distributed data and the Wilcoxon Mann–Whitney test for non-normal distribution. Analysis of variance between multiple data groups was conducted using the Analysis of variance (ANOVA) test for normally distributed data and the Kruskal–Wallis test for non-normally distributed data. Post hoc tests were conducted using the Bonferroni correction. Correlation analysis was performed using Spearman correlation analysis. The diagnostic efficacy of strain parameters was analyzed using receiver operator characteristic (ROC) curves. Inter-observer and intra-observer repeatability tests were conducted using the ICC, with a significance level of  $p < 0.05$  considered statistically significant.

## Results

### Clinical characteristics

The experimental group ( $n = 37$ ) comprised 58.8% males with a mean age of  $56.30 \pm 13.12$  years, while the control group ( $n = 34$ ) consisted of 45.9% males with a mean age of  $51.96 \pm 15.83$  years. The bite sites in the experimental group were all located on the limbs (45.9% on the upper limbs). There was no statistically significant difference between the experimental and control groups in terms of clinical characteristics ( $p > 0.05$ , Table 1). According to the SSS score, there were 25 cases in the mild group, 7 cases in the moderate group, and 5 cases in the severe group. The time interval between the venomous snake bite and hospital consultation was  $9.89 \pm 4.75$  h, and the average length of hospital stay was  $7.17 \pm 3.45$  days, with no statistically significant difference among the three groups ( $p > 0.05$ , Table 1).

### Laboratory indices and electrocardiogram

The levels of serological indicators were all higher in the experimental group than in the control group ( $p < 0.05$ ). The one-way ANOVA test was used to show statistically significant differences in the mean values of WBC count, CRP, and cTnI between the different intoxication groups, and the post hoc multiple comparisons revealed that the WBC count and cTnI in the severe group were significantly higher than those in the mild group ( $p = 0.005$ ,  $p = 0.000$ , Table 2.). Five patients in this study had ECG abnormalities (including ST-T changes in three cases, T-wave inversion in one case, and tachycardia in one case).

### Conventional echocardiographic parameters

The Tei index, which represents the overall function of the myocardium, was significantly different between the control and experimental groups. ( $p = 0.001$ ). The remaining conventional echocardiographic parameters showed no statistically significant difference between the experimental and control groups ( $p > 0.05$ ). The  $E/e'$  ratios of indices assessing left ventricular diastolic function, which were higher than those in the control group, all exceeded normal reference values in the experimental group. However, the difference was not statistically significant ( $p < 0.05$ ). As the severity of the snakebite increased, the LVEF values in the experimental group were within the normal range (Table 3). Micropericardial effusion was observed in two of the patients (Fig. 2).

Characteristics	Healthy Controls	Snakebite patients	Subgroups		
			Mild	Moderate	Severe
Numbers	34	37	25	7	5
Age (y)	51.96 $\pm$ 15.83	56.30 $\pm$ 13.12	51.48 $\pm$ 15.09	52.86 $\pm$ 9.12	51.40 $\pm$ 14.72
Sex (male, %)	20(58.8)	17(45.9)	12(48)	3(42.9)	2(66.7)
BSA (m <sup>2</sup> )	1.63 $\pm$ 0.15	1.62 $\pm$ 0.18	1.61 $\pm$ 0.14	1.68 $\pm$ 0.20	1.66 $\pm$ 0.12
SBP (mmHg)	127.35 $\pm$ 14.96	125.28 $\pm$ 14.10	124.92 $\pm$ 11.49	128.00 $\pm$ 7.46	118.60 $\pm$ 9.10
DBP (mmHg)	78.46 $\pm$ 8.77	76.04 $\pm$ 9.31	77.84 $\pm$ 7.57	82.00 $\pm$ 13.54	76.60 $\pm$ 6.73
Bite site (lower limbs, %)		17(54)	14(56)	3(42.9)	3(60)
Interval between bite and admission (h)		9.89 $\pm$ 4.75	9.89 $\pm$ 3.97	10 $\pm$ 5.15	9.12 $\pm$ 4.45
Average hospitalization days (d)		7.17 $\pm$ 3.45	7.41 $\pm$ 4.26	8.41 $\pm$ 3.02	7.21 $\pm$ 4.02

**Table 1.** Comparison of clinical characteristics in each group. Data are expressed as the Median (IQR). BSA, body surface area; SBP, systolic blood pressure; DBP, diastolic blood pressure.

Characteristics	Healthy Controls(n=34)	Snakebite patients(n=37)	Z/t	p	Mild group(n=25)	Moderate group(n=7)	Severe group(n=5)	H	p
LDH (U/L)	181.35 ± 28.08	221.83 ± 64.57	6.51	0.02	188.000 (170.0,230.0)	242.000 (193.0,244.0)	245.000 (179.0,276.0)	2.489	0.288
CK (U/L)	88.000 (76.5,104.5)	144.000 (105.0,228.0)	-4.473	<0.001	127.000 (95.0,197.0)	177.000 (143.0,239.0)	196.000 (156.0,420.5)	3.984	0.136
CK-MB (ng/mL)	3.050 (2.7,4.1)	3.760 (2.8,5.8)	-1.982	0.048	3.690 (2.6,4.9)	4.140 (3.1,5.9)	9.220 (4.9,9.7)	5.893	0.053
α-HBD(U/L)	96.000 (80.3,116.5)	156.000 (135.5,181.0)	-4.892	<0.001	148.000 (131.0,185.0)	156.000 (147.0,177.0)	159.000 (123.5,169.0)	0.107	0.948
cTnI (ng/L)	0.120 (0.0,0.3)	2.890 (2.2,4.8)	-7.201	<0.001	2.400 (1.5,3.1)*	3.320 (2.6,7.5)	8.120 (5.2,12.6)	12.632	0.002
WBC (× 10 <sup>9</sup> /L)	6.185 (4.6,7.3)	9.530 (6.6,12.4)	-3.503	<0.001	8.420 (6.0,10.1)*	11.040 (6.4,15.8)	13.760 (9.8,19.2)	6.207	0.045
CRP (mg/L)	0.500 (0.5,0.5)	0.500 (0.5,3.0)	-2.958	<0.001	0.500 (0.5,0.7)	0.500 (0.5,5.7)	2.500 (1.5,13.0)	6.500	0.039

**Table 2.** Comparison of laboratory indicators in each group. Data are expressed as the Median (P25, P75). LDH, lactate dehydrogenase; CK, creatine kinase; CK-MB, MB fraction of creatine kinase; α-HBD, alpha-hydroxybutyrate dehydrogenase; cTnI, cardiac troponin I; WBC, white blood cells; CRP, C-reactive protein. \* $p < 0.05$ , compared with the severe group.

Characteristics	Healthy Controls(n=34)	Snakebite patients(n=37)	Z/t	p	Mild group(n=25)	Moderate group(n=7)	Severe group(n=5)	H	p
E/A	1.110 (0.8,1.3)	0.870 (0.8,1.3)	-0.840	0.401	0.910 (0.7,1.4)	0.850 (0.8,0.9)	1.120 (0.6,1.4)	0.488	0.784
E/e'	8.620 (7.1,10.3)	9.480 (8.1,11.4)	-1.571	0.116	9.100 (7.5,11.1)	10.880 (8.9,13.0)	9.870 (8.5,11.7)	1.828	0.401
Tei index	0.420 (0.4,0.5)	0.501 (0.5,0.6)	-3.293	0.001	0.483 (0.4,0.6)	0.501 (0.5,0.6)	0.533 (0.5,0.5)	0.540	0.763
LVEDV (ml)	47.400 (37.2,59.5)	48.000 (41.0,55.3)	-0.610	0.542	48.000 (41.0,59.3)	52.700 (46.8,62.8)	43.800 (35.2,51.1)	1.978	0.372
LVESV (ml)	18.400 (12.6,21.1)	16.300 (11.8,20.1)	-0.804	0.422	17.200 (13.8,21.0)	17.200 (10.5,21.0)	11.500 (11.1,17.4)	2.040	0.361
SV (ml)	29.600 (24.8,39.9)	32.600 (27.7,38.5)	-0.560	0.576	32.700 (26.3,38.0)	37.700 (29.9,45.6)	28.400 (23.9,35.9)	2.057	0.358
CO (l/min)	2.600 (1.8,2.8)	2.100 (2.0,2.8)	-0.633	0.527	2.100 (1.9,2.4)	2.800 (2.2,3.5)	2.000 (1.8,2.8)	3.959	0.138
FS(%)	37.12 ± 3.99	37.03 ± 4.55	0.006	0.936	35.900 (34.1,39.8)	39.200 (33.3,44.0)	34.100 (31.3,41.5)	1.181	0.554
EF(%)	64.900 (61.4,67.7)	65.700 (61.6,71.3)	-0.883	0.377	65.000 (61.0,70.9)	69.500 (61.5,72.6)	70.800 (62.0,72.9)	1.327	0.515

**Table 3.** Comparison of various conventional echocardiographic indexes. Data are expressed as the Median (P25, P75). LVEDV, left ventricular end-diastolic volume; LVESV, left ventricular end-systolic volume; SV, stroke volume; CO, cardiac output; FS, fractional shortening; EF, ejection fraction.  $p < 0.05$ , which is statistically significant.

### Myocardial strain

In both experimental and control groups, ventricular systolic myocardial longitudinal strain showed a gradient: internal layer (GLSendo) > middle layer (GLSmid) > outer layer (GLSepi). Post hoc comparisons using one-way ANOVA showed a decrease in GLSendo with increasing severity of poisoning from pit viper bites, as demonstrated by severe group < moderate group < mild group ( $p = 0.001$ ). The LS myocardial segmentation showed a trend of BLS(basal segment) < MLS(papillary muscle segment) < ALS(apical segment) in both experimental and control groups. We utilized the formula to calculate the RRSR, which was significantly different between the two groups ( $p = 0.001$ ). Furthermore, the experimental group had a lower absolute value of BLS than the control group ( $p = 0.036$ ). In the subgroups with different degrees of intoxication, the mean absolute value of BLS showed a decreasing trend, but the difference was not statistically significant. In the comparison of circumferential strain segments, the ACS and GCS experimental groups were lower than the control group ( $p = 0.014, 0.021$ ), with the severe group showing considerably lower GCS than the mild group. The severity of intoxication was associated with lower absolute values on apical circumferential strain: severe < moderate group < mild group ( $p = 0.022, 0.032$ , respectively). Other strain values, including GLSmid, GLSepi, GLS, MLS, ALS, BCS, and ACS, were not statistically significant in the experimental group compared to the control group, and there was no statistically significant difference between groups with varying degrees of intoxication ( $p > 0.05$ ). (Table 4, Figs. 2 and Fig. 3).

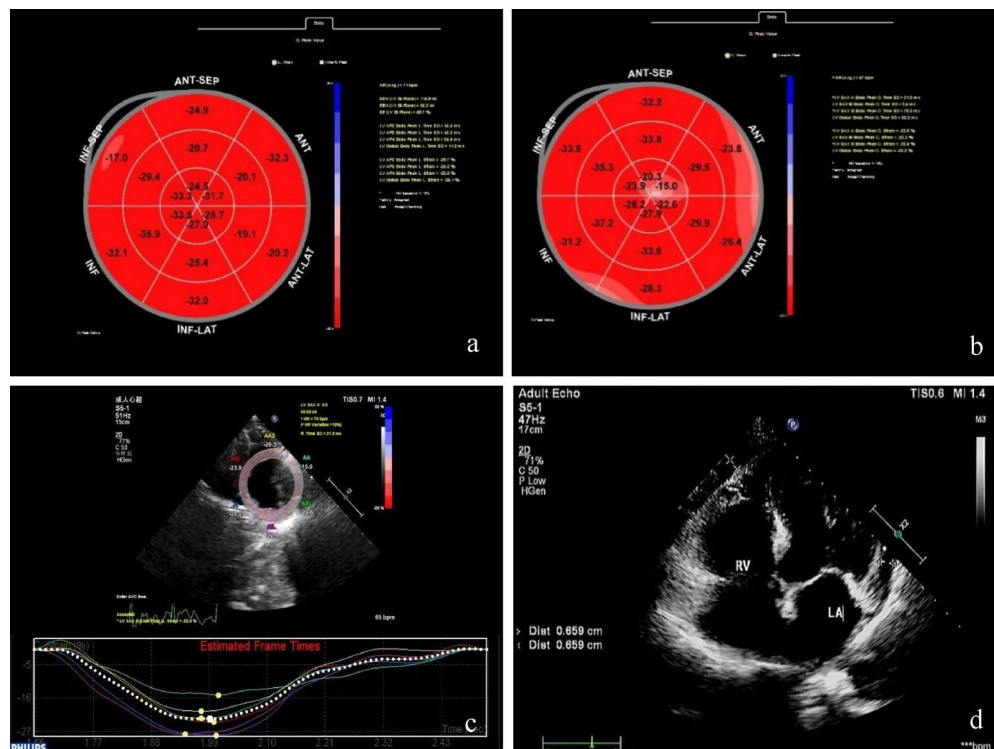


**Fig. 2.** The software offline analysis schematic of left ventricular in QLAB13.0 and pericardial effusion. Light-colored areas indicate reduced longitudinal strain. **(A)** left ventricle after snake bite GLSendo cow eye map; **(B)** BLS decreased after snake bite; **(C)** ACS decreased after snake bite; **(D)** pericardial effusion caused by snake bite. Abbreviations: ANT, indicates anterior; ANT-SEP, anteroseptal; INF-SEP, inferoseptal; INF, inferior; INF-LAT, inferolateral; POST, posterior; ANT-LAT, anterolateral.

### Strain with laboratory indicators

Correlation analysis (Fig. 4) showed that cTnI was moderately negatively correlated with strain parameters including GLSendo, BCS, and GCS ( $r$  values were  $-0.447, -0.427, -0.489$ ,  $p < 0.01$ ). WBC was moderately negatively correlated with MCS, ACS, and GCS ( $r$  values were  $-0.437, -0.593$ , and  $-0.505$ , respectively,  $p < 0.01$ ). CRP showed a mild negative correlation with BCS, GCS, and MLS ( $r$  values were  $-0.331, -0.358$ , and  $-0.331$ , respectively,  $p < 0.05$ ). Creatine Kinase was moderately negatively correlated with GLSendo, BCS, MCS, ACS, and GCS ( $r$  values were  $-0.464, -0.409, -0.411, -0.480, -0.493$ , respectively,  $p < 0.05$ ). Creatine kinase isoenzymes showed a mild negative correlation with GLSendo and ACS ( $r$  values were  $-0.340, -0.393$ ,  $p < 0.05$ ), and showed a moderate negative correlation with BCS and GCS ( $r$  values were  $-0.543, -0.452$ ,  $p < 0.01$ ). GLSendo was positively correlated with GLSepi, BCS, MCS, ACS, and GCS ( $r = 0.389 \sim 0.624$ ,  $p < 0.05$ ). There was no statistically significant correlation between  $\alpha$ -HBD and ultrasound parameters ( $p > 0.05$ ).

### STE predicts cardiotoxicity in pit viper bites

LVEF values were  $> 55\%$  in all 37 patients with pit viper bites in this trial. Using elevated cTnI and/or ischemic electrocardiographic changes after venomous snake bite as criteria for myocardial involvement in venomous snake bites<sup>15–17</sup>, 31 patients were identified as having myocardial injury; ischemic ECG changes included new ST-segment elevation (1 mm), depression (0.5 mm), or T wave inversion (2 mm). Using this criterion for ROC analysis of each strain value, the results showed that GLSendo was the most sensitive indicator for detecting patients with myocardial injury after a pit viper bite. When the absolute value of GLSendo was  $< 18.7$ , the sensitivity of predicting myocardial injury was 0.935, the specificity was 0.833, and the area under the curve (AUC) = 0.933 (Fig. 5).

### Repeatability test

This study analyzed the intra- and inter-observer reliability of each strain parameter (Table 5). ICC values between 0.6 and 0.8 are generally considered to indicate a slightly strong degree of consistency, and those between 0.8 and 1.0 indicate a very strong degree of consistency. In this study, the ICC values for intra-observer variability ranged from 0.853 to 0.950, and the ICC values for inter-observer variability ranged from 0.761 to 0.894, suggesting good reproducibility of inter- and intra-observer strain values measured by 2D-STE.

Characteristics	Healthy Controls (n=34)	Snakebite patients (n=37)	Z/t	p	Mild group (n=25)	Moderate group (n=7)	Severe group (n=5)	H	p
GLS	21.400 (20.0,22.6)	22.300 (20.8,24.2)	-1.710	0.087	22.500 (20.8,24.4)	21.800 (19.3,23.0)	22.200 (17.9,23.6)	2.456	0.293
GLSendo	22.07 ± 1.74	20.79 ± 2.58	4.645	0.035	21.400 (20.3,22.3)†	19.200 (18.9,19.7)	18.500 (17.3,19.4)	16.545	<0.001
GLSmid	16.22 ± 2.02	17.30 ± 2.49	3.219	0.078	17.200 (15.5,19.6)	16.500 (15.3,18.5)	15.800 (15.2,19.3)	0.280	0.869
GLSepi	13.300 (10.6,15.9)	12.300 (10.8,16.4)	-0.380	0.704	13.400 (11.2,18.3)	11.000 (10.2,12.9)	10.700 (10.6,15.4)	5.668	0.059
BLS	18.950 (17.4,21.9)	16.520 (16.1,20.7)	-2.098	0.036	17.800 (16.1,21.0)	20.680 (16.4,21.1)	20.680 (17.9,21.3)	1.737	0.420
MLS	19.150 (18.3,21.1)	19.470 (17.4,20.8)	-0.030	0.976	19.200 (18.1,21.1)	19.470 (17.8,20.8)	19.100 (17.0,20.6)	0.393	0.822
ALS	22.260 (20.2,23.4)	21.400 (18.4,24.4)	-0.517	0.605	21.900 (18.9,23.9)	23.700 (18.4,25.5)	21.420 (19.1,22.1)	1.219	0.544
RRSR	0.560 (0.5,0.6)	0.760 (0.7,1.0)	-3.380	0.001	0.680 (0.5,0.8)	0.680 (0.6,1.0)	0.570 (0.5,0.7)	2.287	0.319
BCS	21.700 (20.9,23.1)	21.900 (20.2,25.6)	-0.323	0.747	22.500 (20.9,27.5)	19.000 (18.8,23.3)	21.100 (18.6,24.3)	6.364	0.042
MCS	23.300 (21.5,25.8)	22.400 (19.5,25.0)	-1.155	0.248	22.600 (20.1,25.9)	19.300 (18.3,27.2)	22.300 (19.9,23.9)	0.712	0.701
ACS	23.700 (21.7,27.4)	19.600 (18.4,24.6)	-2.462	0.014	23.100 (19.0,26.5)†	18.800 (17.0,19.6)	18.300 (16.4,18.9)	10.594	0.005
GCS	24.100 (22.1,26.2)	21.500 (19.4,24.1)	-2.311	0.021	22.400 (21.3,26.0)*	20.100 (19.1,21.5)	19.200 (18.4,20.4)	12.539	0.002

**Table 4.** Comparison of the peak strain parameters in each group. Data are expressed as the Median (P25, P75). GLS, global longitudinal strain; endocardial, mid-layer myocardial and epicardial global longitudinal strain (GLSendo, GLSmid, GLSepi); mean longitudinal strain in the basal, middle, and apical segment (BLS, MLS, and ALS); RRSR, relative regional strain ratio; basal, middle and apical circumferential strain (BCS, MCS, and ACS); GCS, global circumferential strain. \**p* < 0.05, compared with severe group; †*p* < 0.05, between subgroups.

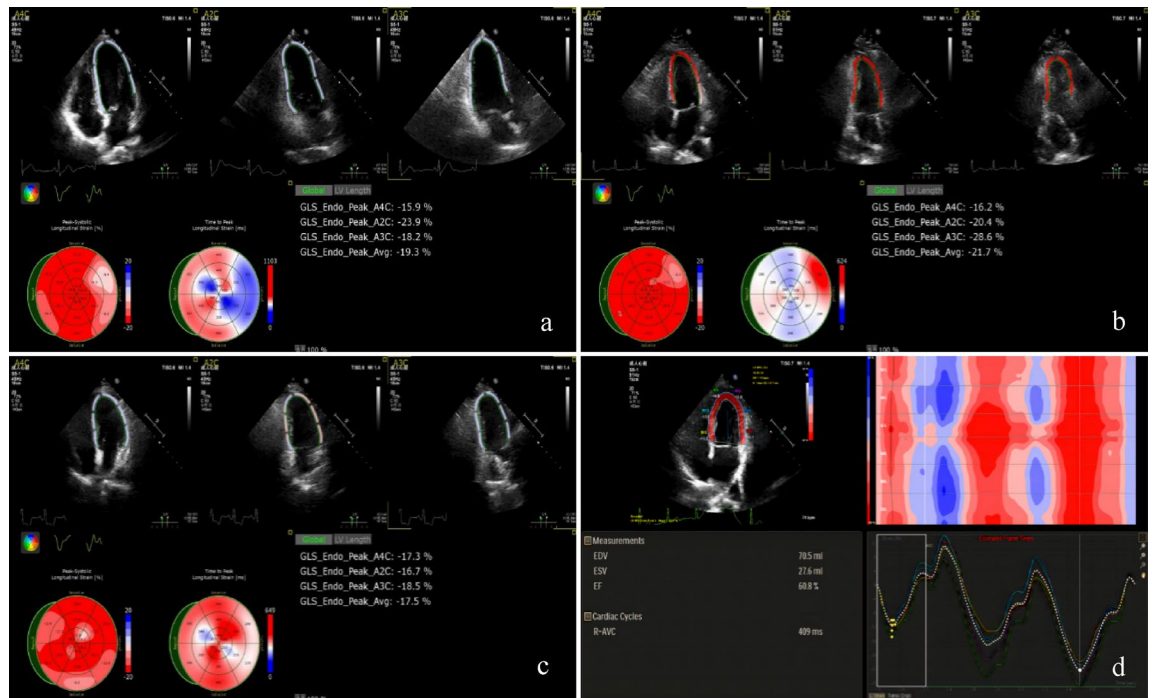
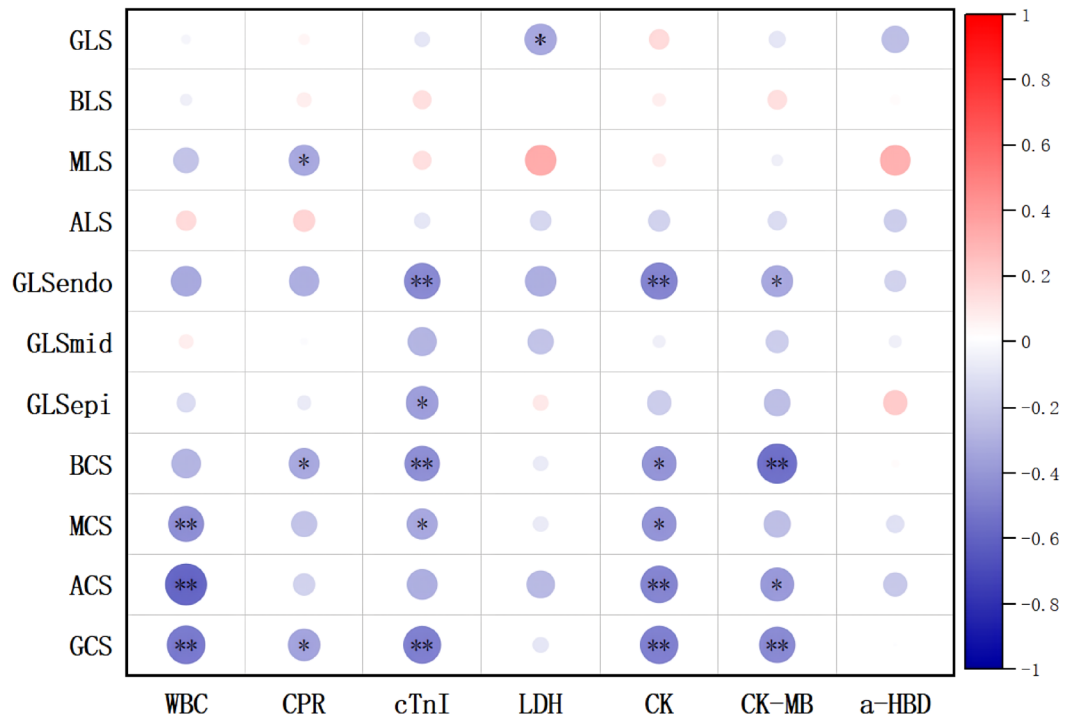


**Fig. 3.** The software offline analysis schematic of the left ventricular GLS in QLAB13.0. (A) Male, 54 years old, mild poisoning, GLS of -21.7%, (B) Female, 43 years old, moderately poisoned, with a GLS of -19.3%, (C) Male, 61, severe poisoning with GLS of -17.5%, (D) Segmental LS decreased after a venomous snake bite. Abbreviations: GLS, endocardial global longitudinal strain; A4C, apical four chamber view; A2C, apical two chamber view; A3C, apical three chamber view.



\* p<0.05 \*\* p<0.01

**Fig. 4.** Schematic diagram of the correlation analysis between strain parameters and laboratory indicators in the software Origin 2021. Serological indicators on the horizontal axis, strain indicators on the vertical axis.

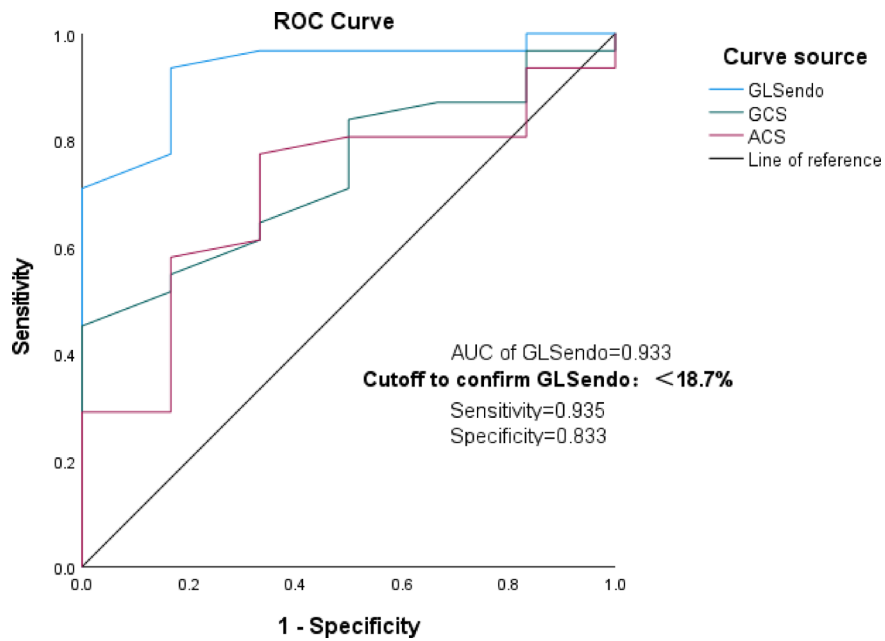


**Fig. 5.** ROC curve of GLSendo, ACS, and GCS predicting myocardial damage after pit viper bite. GLSendo, global longitudinal strain in the endocardial layer, ACS, apical circumferential strain, GCS, global circumferential strain, ROC, receiver operating characteristic curve.

variant	GLPS-A4C	GLPS-A3C	GLPS-A2C	GLS	GLSendo	GLSmid	GLSepi	BCS	MCS	ACS	GCS
Inter-observer (ICC)	0.894	0.775	0.830	0.761	0.770	0.835	0.817	0.840	0.846	0.859	0.853
Intra-observer (ICC)	0.853	0.887	0.876	0.888	0.872	0.946	0.873	0.866	0.923	0.950	0.950

**Table 5.** Inter-observer and intra-observer variation. An ICC value <0.2 indicates poor consistency, 0.2–0.4, fair consistency; 0.4–0.6, moderate consistency; 0.6–0.8, strong consistency; and 0.8–1.0, strong consistency.

## Discussion

### Analysis of serological results

In our study, we found higher levels of cardiac markers than the control group. In the subgroup comparison, the cTnI levels were significantly higher in the severe group compared to the mild group ( $p < 0.01$ ), whereas the differences in cardiac enzyme profiles of LDH, CK, CK-MB, and  $\alpha$ -HBD were not statistically significant between groups. Correlation analysis revealed a strong negative correlation between cTnI and GLSendo, BCS, and GCS. Currently, cTnI has been widely used in clinical practice to monitor myocardial injury following venomous snakebites, and abnormal results indicate an elevated risk of cardiotoxicity. In contrast, there was no correlation between LDH,  $\alpha$ -HBD, and cardiac function parameters. Venom after pit viper bite will lead to local muscular toxicity reaction<sup>18</sup>. Muscle cells swell, become hypoxic, and lyse and release large amounts of cardiac enzyme profile. At that time, Skeletal muscle injury will mask the changes in cardiac enzyme spectral parameters due to myocardial injury, so these parameters cannot be used as specific indicators of myocardial injury.

Snake venom causes a series of allergic inflammatory reactions in the body. CRP concentration is a marker of systemic inflammation<sup>19</sup>. WBC are involved in the immune responses and may modulate and respond to the severity of inflammation<sup>20</sup>. Marked infiltration of WBC into localized snakebites is an important feature of inflammation triggered by viper venom. In this study, CRP and WBC were significantly higher in the experimental group than in the control group. WBC and CRP showed some correlation with the values of several strain parameters, demonstrating that cardiomyocytes may be involved in this series of anaphylactic reactions. Langhorn et al. proposed that the systemic inflammatory response induced by venom toxins has secondary deleterious effects on the myocardium, which in turn leads to myocardial injury<sup>21</sup>. The mechanisms of myocardial injury caused by inflammatory disease states include hemodynamic changes, microvascular thrombosis, and the toxic effects of cytokines<sup>22,23</sup>.

### Analysis of results of conventional ultrasound parameters

Conventional echocardiographic structural and functional parameters in the control and experimental groups in this study were within the normal range and the differences were not statistically significant in the different groups, making it difficult to respond sensitively and specifically to cardiotoxic injury<sup>24</sup>, while Santos et al. found that the effect of low-dose snake venom on myocardial contractility was transient and mild<sup>25</sup>. Lang et al. proposed that conventional echocardiographic parameters are less sensitive in detecting myocardial injury with preserved LVEF, especially when changes are limited to a few segments<sup>26</sup>. However, conventional echocardiography is very intuitive for the observation of pericardial effusion. Hemorrhagic toxins in the venom of the snake contain metalloproteinases and kinases, which can directly disrupt the endothelium of the vessels to increase vascular permeability. In the present study, two patients with micro pericardial effusion were identified.

The Tei index reflects changes in tissue motion and is less susceptible to blood flow loading than the LVEF. Its reduced heterogeneity is more likely to indicate differences in regional wall stress, apoptosis, or fibrosis<sup>27</sup>. It is a clinically meaningful diagnostic and prognostic parameter that is widely used in the study of heart failure, acute myocardial infarction, dilated cardiomyopathy, etc.<sup>28</sup>. In this study, the Tei index was elevated in the experimental group compared to the control group, indicating a decrease in overall left heart function. The E/e' ratio is a well-recognized marker of elevated left ventricular diastolic dysfunction and also has advantages in revealing cardiotoxicity<sup>29</sup>. In the present study, the E/e' ratios of the experimental group were all greater than 9, which exceeded the normal reference value and was higher than that of the control group, but the differences were not statistically significant ( $p < 0.05$ ). Follow-up studies could further expand the sample size to discuss the changes in left heart diastolic function after snakebite.

### Analysis of myocardial strain findings

The left ventricular myocardium consists of obliquely walking epicardial myofibers, circularly walking mid-myocardial fibers, and longitudinally walking endocardial myofibers<sup>30</sup>. The radial curvature and orientations of the myocardial radius from layer to layer, result in differences in the effect of myocardial tone on cardiac function in each layer. In this study, both the experimental and control groups showed a gradient trend of GLSendo > GLSmid > GLSepi, with statistically significant variations across each layer. This result is probably because the left ventricle is composed of approximately 70% longitudinal muscle, whereas the endocardial layer is primarily responsible for it. However, the endocardium was also more susceptible to injury due to its relatively high energy demand. Analysis of variance showed that the absolute value of GLSendo in the experimental group was significantly lower than that in the control group, and decreased significantly with increasing intoxication, but the differences in GLS, GLSmid, and GLSepi were not statistically significant in any of the groups. Consistent with this result, previous studies demonstrated that low and medium doses of pit viper venom induced irregular shape of myocardial fibers, and mitochondrial swelling in mice, which manifested as focal lesions in the endocardium of the ventricles, and involved the middle and epicardium sequentially with the severity of ischemia<sup>31,32</sup>. The inner myocardial capillaries are denser and more distant from the coronary arteries, making

them the most susceptible to hypoperfusion and ischemia, so early cardiotoxicity is characterized by a decline in longitudinal endocardial function<sup>33</sup>.

We found that both the experimental group and the control group showed a pattern of change of BLS < MLS < ALS, which is consistent with the pattern of gradual shortening of myocardial fibers along the long axis from apical to basal during cardiac contraction<sup>34</sup>, and the absolute value of BLS was significantly decreased in the experimental group relative to the control group strain. RRSR has a diagnostic value for myocardial injury with apical retention of long-axis strain, which is a measure of the relative degree of apical retention of longitudinal strain, and it is widely used in the clinic to diagnose cardiac amyloidosis, a type of apical retention of myocardial injury, which is sensitive and specific<sup>35</sup>. In our study, the RRSR of the experimental group was significantly higher than that of the control group, which indicated that the basal and mid segments of the experimental group declined more significantly compared with the apical segment, so we hypothesized that the basal segment of the left ventricular long-axis strain was the first to be involved after viper bite, and the possible mechanism is that the basal segment of the ventricle is continuous with longitudinal subendocardial muscle fibers that are sensitive to ischemia, and the effects of toxins on the cardiovascular system are more pronounced in the basal segment than in the apical segment.

The circumferential strain parameters, including ACS and GCS, were significantly lower in the experimental group compared to the control group, suggesting that the snake venom may have affected the middle myocardium. The apical segments showed the largest circumferential strain due to their role in ensuring maximum energy efficiency of pumping during systole. Any abnormality in circumferential strain would first manifest in the apical segments<sup>36</sup>.

### Predictors of myocardial injury after venomous snake bite

ROC curve analysis showed that GLSendo was a highly sensitive and specific predictor for detecting high-risk patients with pit viper bite-related myocardial injury. The combination of high-sensitivity troponin and GLS may provide the greatest sensitivity and negative predictive value for predicting future cardiotoxicity<sup>37</sup>. However, there is no uniform clinical definition of cardiotoxicity in snakebite patients, and further studies are needed to support this evidence. The experimental group included in this study had normal LVEF and none of them showed any relevant clinical symptoms, which may be indicative of subclinical cardiotoxicity in these snakebite patients.

### Limitations

This study might encompass potential biases inherent in the assessment of cardiac function at discrete time points via echocardiographic and serologic indices. The modest sample dimension and abbreviated surveillance duration for each participant obviate the capacity for prognostic appraisal regarding the evolution of GLS in snakebite patients. Nonetheless, preliminary alterations were discerned, including the delineation of cases exhibiting an abnormal Tei index, which may be subjected to subsequent examinations to elucidate associations between diastolic functional modulations and strain in snakebite victims. Moreover, this inquiry was constrained to envenomation events involving a singular species of venomous snake; forthcoming studies may opt to incorporate additional varieties of poisonous snakes to broaden the understanding of myocardial damage.

### Conclusions

In the context of viper envenomation, specifically from pit vipers such as the *Protobothrops mucrosquamatus*, 2D-STE has been employed to evaluate myocardial function. GLS has demonstrated a significant correlation with cardiac biomarker profiles post-envenomation. This strain parameter is considered more sensitive and specific for the early detection of venom-induced cardiotoxicity compared to conventional echocardiographic parameters and serum biomarkers. GLS, as an early diagnostic tool, allows for precise monitoring of myocardial dysfunction, enabling healthcare providers to gauge the severity of toxicity and implement appropriate interventions promptly, thus improving patient outcomes following pit viper envenomation.

### Data availability

The datasets generated during and/or analysed during the current study are available from the corresponding author on reasonable request.

Received: 21 August 2024; Accepted: 20 June 2025

Published online: 01 July 2025

### References

1. Simões, L. O. et al. Cardiac effect induced by *Crotalus durissus* cascavella venom: Morphofunctional evidence and mechanism of action. *Toxicol. Lett.* **337**, 121–133 (2021).
2. Liblik, K. et al. Snakebite envenomation and heart: Systematic review. *Curr. Probl. Cardiol.* **47**, 100861 (2022).
3. Zamorano, J. L. et al. 2016 ESC position paper on cancer treatments and cardiovascular toxicity developed under the auspices of the ESC committee for practice guidelines: The task force for cancer treatments and cardiovascular toxicity of the European society of cardiology (ESC). *Eur. Heart J.* **37**, 2768–2801 (2016).
4. Stanton, T., Leano, R. & Marwick, T. H. Prediction of all-cause mortality from global longitudinal speckle strain: Comparison with ejection fraction and wall motion scoring. *Circ. Cardiovasc. Imaging* **2**, 356–364 (2009).
5. Santoro, C. et al. 2D and 3D strain for detection of subclinical anthracycline cardiotoxicity in breast cancer patients: A balance with feasibility. *Eur. Heart J. Cardiovasc. Imaging* **18**, 930–936 (2017).
6. Sawaya, H. et al. Early detection and prediction of cardiotoxicity in chemotherapy-treated patients. *Am. J. Cardiol.* **107**, 1375–1380 (2011).

7. Tsai, W.-C. et al. Diagnostic value of segmental longitudinal strain by automated function imaging in coronary artery disease without left ventricular dysfunction. *J. Am. Soc. Echocardiogr.* **23**, 1183–1189 (2010).
8. Plana, J. C. et al. Expert consensus for multimodality imaging evaluation of adult patients during and after cancer therapy: A report from the American society of echocardiography and the European association of cardiovascular imaging. *J. Am. Soc. Echocardiogr. Off. Publ. Am. Soc. Echocardiogr.* **27**, 911–939 (2014).
9. Roly, Z. Y., Islam, M. M. & Reza, M. A. A comparative in silico characterization of functional and physicochemical properties of 3FTx (three finger toxin) proteins from four venomous snakes. *Bioinformation* **10**, 281 (2014).
10. John, B. A., Kumar, M. A., Gunasekaran, K. & Iyadurai, R. Cardiovascular manifestations and patient outcomes following snake envenomation: A pilot study. *Trop. Doct.* **49**, 10–13 (2019).
11. Dart, R. C., Hurlbut, K. M., Garcia, R. & Boren, J. Validation of a severity score for the assessment of crotalid snakebite. *Ann. Emerg. Med.* **27**, 321–326 (1996).
12. Nagueh, S. F. et al. Recommendations for the evaluation of left ventricular diastolic function by echocardiography: An update from the American society of echocardiography and the European association of cardiovascular imaging. *J. Am. Soc. Echocardiogr.* **29**, 277–314 (2016).
13. Risum, N. et al. Variability of global left ventricular deformation analysis using vendor dependent and independent two-dimensional speckle-tracking software in adults. *J. Am. Soc. Echocardiogr.* **25**, 1195–1203 (2012).
14. Collier, P., Phelan, D. & Klein, A. A test in context: Myocardial strain measured by speckle-tracking echocardiography. *J. Am. Coll. Cardiol.* **69**, 1043–1056 (2017).
15. Senthilkumaran, S., Meenakshisundaram, R. & Thirumalaikolundusubramanian, P. Cardiac tamponade in russell viper (*Daboia russelii*) bite case report with brief review. *J. Emerg. Med.* **42**, 288–290 (2012).
16. Lawler, J. B., Frye, M. A., Bera, M. M., Ehrhart, E. J. & Bright, J. M. Third-degree atrioventricular block in a horse secondary to rattlesnake envenomation. *J. Vet. Intern. Med.* **22**, 486–490 (2008).
17. Moon, J. M. et al. The effect of myocardial injury on the clinical course of snake envenomation in South Korea. *Clin. Toxicol.* **59**, 286–295 (2021).
18. Gutiérrez, J. M. et al. Snakebite envenoming. *Nat. Rev. Dis. Primer* **3**, 17063 (2017).
19. Ferreira, J. P. et al. High-sensitivity C-reactive protein in heart failure with preserved ejection fraction: Findings from TOPCAT. *Int. J. Cardiol.* **402**, 131818 (2024).
20. Ngwenyama, N. et al. Isolevuglandin-modified cardiac proteins drive CD4+ T-cell activation in the heart and promote cardiac dysfunction. *Circulation* **143**, 1242–1255 (2021).
21. Langhorn, R. et al. Myocardial injury in dogs with snakebites and its relation to systemic inflammation: Myocardial injury in dogs with snakebites. *J. Vet. Emerg. Crit. Care* **24**, 174–181 (2014).
22. Watts, E. R. & Walmsley, S. R. Inflammation and hypoxia: HIF and PHD isoform selectivity. *Trends Mol. Med.* **25**, 33–46 (2019).
23. Tanaka, T., Narazaki, M. & Kishimoto, T. Immunotherapeutic implications of IL-6 blockade for cytokine storm. *Immunotherapy* **8**, 959–970 (2016).
24. Santos, W. S. et al. Proteomic analysis reveals rattlesnake venom modulation of proteins associated with cardiac tissue damage in mouse hearts. *J. Proteomics* **258**, 104530 (2022).
25. Negishi, K. et al. Independent and incremental value of deformation indices for prediction of trastuzumab-induced cardiotoxicity. *J. Am. Soc. Echocardiogr. Off. Publ. Am. Soc. Echocardiogr.* **26**, 493–498 (2013).
26. Lang, R. M. et al. Recommendations for cardiac chamber quantification by echocardiography in adults: An update from the American society of echocardiography and the European association of cardiovascular imaging. *Eur. Heart J. Cardiovasc. Imaging* **16**, 233–270 (2015).
27. Meric, M. et al. Tissue doppler myocardial performance index in patients with heart failure and its relationship with haemodynamic parameters. *Int. J. Cardiovasc. Imaging* **30**, 1057–1064 (2014).
28. Zhong, Y. et al. Assessment of left ventricular dissipative energy loss by vector flow mapping in patients with end-stage renal disease. *J. Ultrasound Med.* **35**, 965–973 (2016).
29. Johansen, N. D., Biering-Sørensen, T., Jensen, J. S. & Mogelvang, R. Diastolic dysfunction revisited: A new, feasible, and unambiguous echocardiographic classification predicts major cardiovascular events. *Am. Heart J.* **188**, 136–146 (2017).
30. Buckberg, G. D. Basic science review: The helix and the heart. *J. Thorac. Cardiovasc. Surg.* **124**, 863–883 (2002).
31. Sengupta, P. P. et al. Left ventricular form and function revisited: Applied translational science to cardiovascular ultrasound imaging. *J. Am. Soc. Echocardiogr. Off. Publ. Am. Soc. Echocardiogr.* **20**, 539–551 (2007).
32. Shi, J., Pan, C., Kong, D., Cheng, L. & Shu, X. Left ventricular longitudinal and circumferential layer-specific myocardial strains and their determinants in healthy subjects. *Echocardiogr. Mt. Kisco N* **33**, 510–518 (2016).
33. Kang, Y. et al. Two-dimensional speckle tracking echocardiography combined with high-sensitive cardiac troponin T in early detection and prediction of cardiotoxicity during epirubicin-based chemotherapy. *Eur. J. Heart Fail.* **16**, 300–308 (2014).
34. Serri, K. et al. Global and regional myocardial function quantification by two-dimensional strain: application in hypertrophic cardiomyopathy. *J. Am. Coll. Cardiol.* **47**, 1175–1181 (2006).
35. Senapati, A. et al. Prognostic implication of relative regional strain ratio in cardiac amyloidosis. *Heart Br. Card. Soc.* **102**, 748–754 (2016).
36. Leitman, M. et al. Circumferential and longitudinal strain in 3 myocardial layers in normal subjects and in patients with regional left ventricular dysfunction. *J. Am. Soc. Echocardiogr. Off. Publ. Am. Soc. Echocardiogr.* **23**, 64–70 (2010).
37. Sawaya, H. et al. Assessment of echocardiography and biomarkers for the extended prediction of cardiotoxicity in patients treated with anthracyclines, taxanes, and trastuzumab. *Circ. Cardiovasc. Imaging* **5**, 596–603 (2012).

## Acknowledgements

We thank Professor Shuqing Yang of the Emergency Department of Chongqing Emergency Medical Center for his assistance in patient collection and identification of snake species.

## Author contributions

Conception and design of the experiment: J.C., Y.F. and C.J.Y.; data collection: J.C., Y.F., C.M.Y. and J.Q.C.; reference search and procurement: J.C., Y.F. and J.M.X.; analysis of data: J.C., Y.F., J.Q.C. and L.Q.S.; figure generation: J.C., J.M.X. and L.F.; interpretation of data: C.J.Y. and J.C.; writing the first draft: J.C., Y.F., L.Q.S. and C.J.Y. revision of the manuscript: all authors. All authors have read and approved the final version of the manuscript.

## Funding

This study has received funding by Chongqing Medical Scientific Research Project (Joint project of Chongqing Health Commission and Science and Technology Bureau, 2023MSXM097) and the Program for Youth Innovation in Future Medicine, Chongqing Medical University (W0114).

## Declarations

### Competing interests

The authors declare no competing interests.

### Additional information

**Correspondence** and requests for materials should be addressed to C.Y.

**Reprints and permissions information** is available at [www.nature.com/reprints](http://www.nature.com/reprints).

**Publisher's note** Springer Nature remains neutral with regard to jurisdictional claims in published maps and institutional affiliations.

**Open Access** This article is licensed under a Creative Commons Attribution-NonCommercial-NoDerivatives 4.0 International License, which permits any non-commercial use, sharing, distribution and reproduction in any medium or format, as long as you give appropriate credit to the original author(s) and the source, provide a link to the Creative Commons licence, and indicate if you modified the licensed material. You do not have permission under this licence to share adapted material derived from this article or parts of it. The images or other third party material in this article are included in the article's Creative Commons licence, unless indicated otherwise in a credit line to the material. If material is not included in the article's Creative Commons licence and your intended use is not permitted by statutory regulation or exceeds the permitted use, you will need to obtain permission directly from the copyright holder. To view a copy of this licence, visit <http://creativecommons.org/licenses/by-nc-nd/4.0/>.

© The Author(s) 2025